




Soil erosion in relation to land-use changes in the sediments of Amik Lake near Antioch antique city during the last 4 kyr

The Holocene
1–15
© The Author(s) 2017
Reprints and permissions:
sagepub.co.uk/journalsPermissions.nav
DOI: 10.1177/0959683617715702
journals.sagepub.com/home/hol


El Ouahabi Meriam,¹ Hubert-Ferrari Aurélia,² Lebeau Héléne,² Karabacak Volkan,³ Vander Auwera Jacqueline,⁴ Lepoint Gilles,⁵ Dewitte Olivier⁶ and Schmidt Sabine⁷

Abstract

The Amik Basin in the Eastern Mediterranean region occupied since 6000–7000 BC has sustained a highly variable anthropic pressure culminating during the late Roman Period when the Antioch city reached its golden age. The present 6-m-long sedimentary record of the Amik Lake occupying the central part of the Basin constrains major paleoenvironmental changes over the past 4000 years using multi-proxy analyses (grain size, magnetic susceptibility, and x-ray fluorescence (XRF) geochemistry). An age model is provided by combining short-lived radionuclides with radiocarbon dating. A lake/marsh prevailed during the last 4 kyr with a level increase at the beginning of the Roman Period possibly related to optimum climatic condition and water channeling. The Bronze/Iron Ages are characterized by a strong terrigenous input linked to deforestation, exploitation of mineral resources, and the beginning of upland cultivation. The Bronze/Iron Age transition marked by the collapse of the Hittite Empire is clearly documented. Erosion continued during the Roman Period and nearly stopped during the early Islamic Period in conjunction with a decreasing population and soil depletion on the calcareous highland. The soil-stripped limestone outcrops triggered an increase in CaO in the lake water and a general decrease in ZrO₂ released in the landscape that lasts until the present day. During the Islamic Period, pastoralism on the highland sustained continued soil erosion of the ophiolitic Amanus Mountains. The Modern Period is characterized by a higher pressure particularly on the Amanus Mountains linked to deforestation, road construction, ore exploitation, and drying of the lake for agriculture practices.

Keywords

Amik Lake, Antioch city, chemistry, core sediments, land use, late Holocene, soil erosion, Southern Turkey

Received 9 May 2017; revised manuscript accepted 19 May 2017

Introduction

Over millennia, food security, human health, urbanization, water and soil quality, runoff, and sedimentation are the triggering factors of the land-use changes. The landscape is indeed modified through agricultural activity, logging, and grazing. These anthropogenic impacts depend on social, political, economic, and even cultural and religious factors complemented by climatic changes. Climatic variations strongly impact land use and might have caused the collapse of ancient civilizations (e.g. Grove, 1996; Kuzucuoğlu and Tsirtsoni, 2016; Margaris et al., 1996; Wick et al., 2003). The related abandonment of agricultural land can then significantly alter sediment dynamics on a regional scale. Anthropogenic and climatic factors are thus strongly untangled over the long term regarding landscape evolution, especially in the Mediterranean region (Nunes et al., 2008).

The Mediterranean and the Middle East represent an environment that has supported an agricultural way of life for more than 10 millennia. This environment has repeatedly been described as degraded, suggesting conceptual confusion between transformation and destruction (e.g. Dunjo et al., 2003; Kosmas et al., 1997; Naveh and Dan, 1973; Van Andel et al., 1990). To address issues as complex as land degradation in regions where men lived and farmed over 10,000 years and its relation with landscape evolution,

one must integrate systematically environmental change and land use with archaeological investigations (i.e. Butzer, 2005).

In this study, we focus on the Amik (Amuq) plain located in southern Turkey near the Syrian border, 50 km east of the Mediterranean Sea. The Amik Basin has a long human history, associated

¹U. R. Argiles, Géochimie et Environnements, Department of Geology, University of Liège, Belgium

²Department of Geography, University of Liège, Belgium

³Department of Geological Engineering, Eskisehir Osmangazi University, Turkey

⁴Pétrologie, Géochimie et Pétrophysique, Department of Geology, University of Liège, Belgium

⁵Département des Sciences et Gestion de l'Environnement, University of Liège, Belgium

⁶Department of Earth Sciences, Royal Museum for Central Africa, Belgium

⁷CNRS, EPOC, UMR5805, Université de Bordeaux, France

Corresponding author:

El Ouahabi Meriam, U. R. Argiles, Géochimie et Environnements, Department of Geology, University of Liège, Liège 4000, Belgium.
Email: meriam.elouahabi@ulg.ac.be

with dense, variable, and marked human settlements. The latter, started probably since the Neolithic time (Braidwood and Braidwood, 1960), is marked during the Bronze Age by the development of the Alalakh, the capital of a regional state (Yener and Wilkinson, 2007), and later by the rise of the antique Antioch city, the third largest city of the Roman Empire (~500,000 inhabitants; De Giorgi, 2007). In 1920, there were only about 180,000 people living in the region, and presently, Antakya (ancient Antioch) has a population of only 250,000 inhabitants (Doğruel and Leman, 2009). The Amik region had thus undergone a highly variable human occupation. It is thus a particularly interesting laboratory regarding the human impacts on the landscape in the Mediterranean region.

The history of the Amik region has been well documented. The region was home to several major archaeological excavations. During the 1930s and 1950s (Braidwood and Braidwood, 1960; Haines, 1971), the archaeological studies focused on the Amik Basin. Starting in 1995, excavations were renewed by the Oriental Institute (Chicago University) as the Amuq Valley Regional Projects (AVRP) in order to better understand the settlement pattern and the systems of land use through an interdisciplinary regional research program from the Chalcolithic to the Islamic Period (e.g. Yener, 2005, 2010; Yener et al., 2000). The defined stratigraphical sequences and the associated artifact typology found in the Amik plain are presently a standard reference for chronologies and material cultures in all the neighboring regions (Yener et al., 2000).

The present sedimentological study was undertaken in the eastern part of the Amik Lake near the junction with the Afrin River. The presently dried lake occupied the central part of the Amik Basin, a tectonic pull-apart basin. Our aim was to constrain environmental changes during the last 4000 years in relation to the different human occupation phases. The regional tectonics dominated by the Dead Sea Fault Zone (DSFZ), as well as the settlement and land-use histories since the Bronze Age, were first rapidly reviewed because they provided a necessary framework for the interpretation of the data. The analysis of an ~6-m sedimentary sequence is then presented using a multi-proxy approach (magnetic susceptibility (MS), grain size, x-ray fluorescence (XRF) geochemistry, and organic geochemistry). The age of the sequence was constrained by short-lived radioisotopes and radiocarbon dating and tie points using historical earthquakes that let a fingerprint. The results were discussed considering the different geoarchaeological data available in the area.

Regional, tectonic, and geological setting of the Amik Basin

The 50-km-long and 50-km-wide Amik plain is a tectonic basin filled by up to 2.5-km-thick Plio-Quaternary sediments (Gülen et al., 1987) and crossed by the Dead Sea Fault (DSF). The DSF is composed of two segments, the Karasu Fault to the north bounding of the Amanus Mountain and the Hacıpasa Fault to the south in the Orontes valley (Akyüz et al., 2006; Altunel et al., 2009; Karabacak and Altunel, 2013; Karabacak et al., 2010; Figure 1). The two active left-lateral strike-slip faults defined a pull-apart structure and have ruptured in large destructive earthquakes during historical time (e.g. Akyüz et al., 2006).

The basin is surrounded by several mountains and plateaus. To the west stands the Amanus Mountains that culminates at 2250 m and is made of sedimentary and metamorphic rocks as well as of a large ophiolitic body (Boulton et al., 2007). To the south lies the low ranges of calcareous Jebel al-Aqra or Kuseyr Plateau. To the northeast, the Kurt Mountains culminating at 825 m are mostly composed of metamorphic rocks (Altunel et al., 2009; Eger, 2011; Karabacak and Altunel, 2013; Parlak et al., 2009; Robertson, 2002; Wilkinson, 2000).

The plain is watered by three large rivers: the Orontes, the Karasu, and the Afrin. Its central part used to be occupied by

wetlands and a large shallow lake (Figures 1 and 2). The lake has a complex history with alternating extension and disappearance partly unraveled by geoarchaeological studies (Casana, 2008; Friedman et al., 1997; Wilkinson, 1997; Wilkinson, 2000). A lacustrine environment is attested around 7500 years ago until the early Bronze Age sites (Schumm, 1963; Wilkinson, 2000). Between 3000 and 1000 BC, a drying of the lake is attested by soil development and accumulation of calcium carbon at the center of the lake (Casana, 2008; Wilkinson, 1999). During the Roman Period, the environment was again more humid, and the lake surface increased to reach a maximum extent during the first millennium AD (Casana, 2007; Eger, 2011; Wilkinson, 1997). During the 19th century and the mid-20th century, the lake was the main resource for the local economy, and it was artificially drained at the beginning of the 1940s (Çalışkan, 2008); the desiccation work was completed in 1987 (Kilic et al., 2006).

Settlement and land-use histories

The three rivers draining the Amik Basin form a particularly fertile environment in which continuous human occupation is attested since about 6000–7000 BC (e.g. Eger, 2011). The low-lying Amik plain was already well occupied during Chalcolithic with a settlement concentration in the central part of the plain. Starting in the Bronze Age, settlement dispersal occurred in different phases very briefly summarized here (Casana, 2007; Wilkinson, 2000). Starting around 3000 BC during the Bronze Age, sites spread to the outskirts of the plain with a concentration along an east–west corridor along the southern part of the plain, which is inferred to represent an interregional route system (Batiuk, 2005). In the Iron Age, during the first millennium BC, the tell-based settlement pattern continued its transformation to a more dispersed pattern of numerous small settlements associated with the occupation of some upland (i.e. valleys in the Jebel al-Aqra Mountain to the south of the Amik Lake; Batiuk, 2005; Casana, 2003; Casana and Wilkinson, 2005). A third phase of more intensive occupation started during the Hellenistic Period (300 BC) and ended around AD 650 during the late Roman Period. The period is characterized by the conversion of upland areas to intensive agricultural production (Wilkinson, 1997; 2000), starting probably around AD 50 by the systematic channelization of the rivers flowing into the Amik Basin and to the south into the Ghab Basin (Wilkinson and Rayne, 2010). The intensive agricultural farming and irrigation network that developed around the Amik Basin were necessary to feed the large population of the Antioch city. The city was one of the largest in the Roman Empire, with maybe up to 500,000 inhabitants including its suburbs (De Giorgi, 2007). In fact, during the late Roman Period, the Amik plain was more densely occupied than at any time in its history (Casana, 2008). The related intensive land use created the necessary preconditions for severe soil erosion to occur, but there was a long time lag between the initial settlement of upland areas starting around 300 BC and the first evidence of soil erosion occurred after AD 150 (Casana, 2008). Casana (2008) inferred that the late Roman soil erosion created widespread floodplain aggradation and rapid siltation of the man-constructed canals and transformed the fertile Amik plain to unproductive marshland. After AD 700, there was a progressive decrease in population and settlement contemporary with the decline in the Antioch city.

Material and methods

Sampling site

The site (36°20.655'N–036°20'.948'E) is located just at the border of the Kumtepe village near the eastern border of the

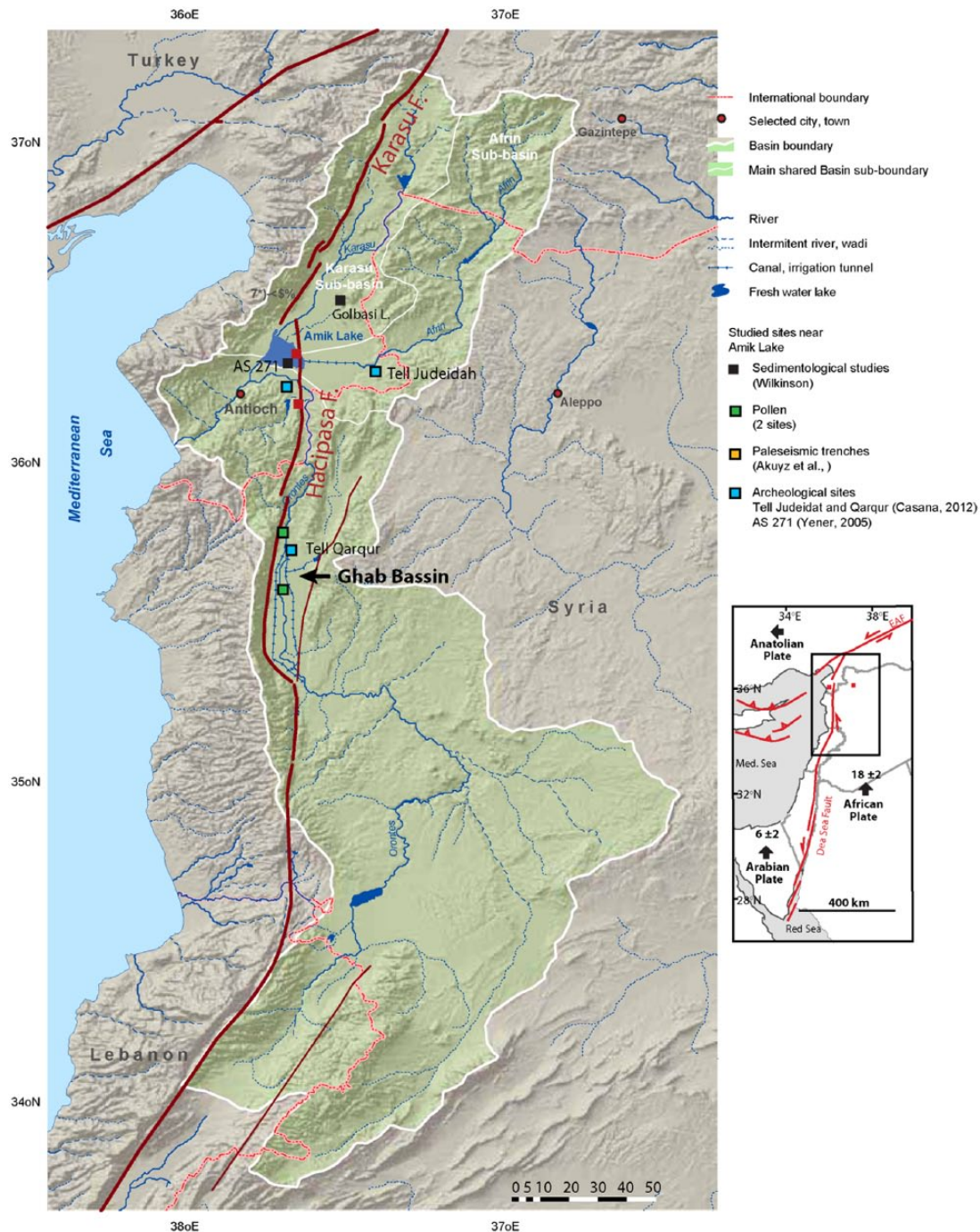


Figure 1. Geomorphological situation of the Amik Lake, the studied pollen record sites, the nearest archaeological sites, the sedimentological study, and the paleoseismological trenches.

lake defined by a low sandy ridge containing lake roman pottery and shells (Casana, 2008; Figures 1 and 2). On this side of the lake, the main water inflow is provided by the Afrin River, which drains a large part of the calcareous Arabian Province (Figure 1). The site stands near the northern extremity of the Hacıpasa Segment of the DSF where a large tectonic subsidence is expected (Karabacak et al., 2010) with respect to the central part of the lake previously studied by Wilkinson (2005; Figures 1 and 2). It is adjacent to significant archaeological remains, such as the Kara Tepe tell (AS86) located ~800 m to the east (Braidwood et al., 1981), and the large Bronze settlement (Yener et al., 2000) also occupied during the late Roman Period. The sampling site is finally very proximal to the Roman canal A (north) of the Afrin River (Yener et al., 2000; Figure 2). Sediments were collected in a trench every 1 cm during the summer time (1 July 2012) until reaching the water table at a

depth of 1.5 m. The sampling was extended to 6 m depth, thanks to a spindle-type drilling machine with mechanical and hydraulic transmission.

Methods

Different types of sedimentological analyses were performed to highlight the occurrence of significant environmental changes. MS performed every centimeter was used as a first indicator of input of terrigenous materials, allochthonous to the lake. It was completed by grain-size measurement at the same resolution on bulk samples using a laser diffraction particle analyzer Malvern Mastersizer 2000 at the University of Liège (Belgium). In addition, organic and inorganic geochemistry was performed at a lower resolution (every 5 and 10 cm at the core bottom). The total organic carbon (TOC) and

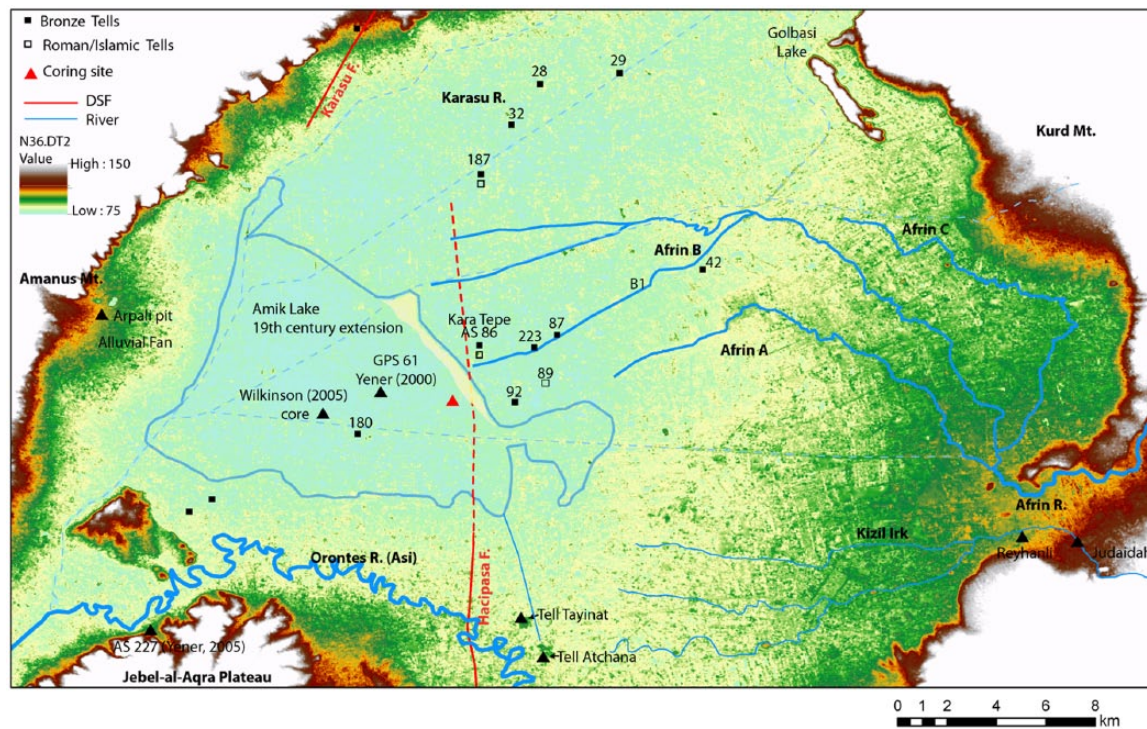


Figure 2. Map illustrating the location of all archaeological sites in the Amik plain (southern Turkey) with evidence of Paleolithic, Iron, Bronze, and Roman Age occupation. The largest sites are indicated by the survey number assigned by the Amuq Valley Regional Project (Casana and Wilkinson, 2005). Wilkinson (2005) studied core sediments located in the present map.

carbon and nitrogen isotopes were used to discriminate between the allochthonous and the autochthonous organic input to the lake (Meyers and Teranes, 2001; Talbot and Livingstone, 1989). Major (Si, Ti, Al, Fe, Mn, Mg, Ca, Na, and K) and trace elements above 500 ppm (Ba, Cr, Cu, Ni, Sr, Rh, P, Zr, and Zn) were scanned using XRF spectrometry (ARL 9400 sequential XRF XP, University of Liège). The amount of the following oxide form was computed: SiO_2 , TiO_2 , Al_2O_3 , Fe_2O_3 , MnO , MgO , CaO , Na_2O , K_2O , ZrO_2 , ZnO , NiO , Cr_2O_3 , and SrO . Variations in ZrO_2 , Cr_2O_3 , NiO , and ZnO were used to estimate changes in soil erosion induced mostly by human occupation. Indeed, zirconium is generally considered as a reliable index upon which to base quantitative evolution of pedogenic changes in the sediments (Sudom and Arnaud, 1971). Cr_2O_3 , NiO and ZnO contents provide insight into the soil erosion of phiolitic rocks in the Amanus Mountains.

The degree of alteration in the catchment using the chemical index of alteration (CIA) was evaluated, where $\text{CIA} = [\text{Al}_2\text{O}_3 / (\text{Al}_2\text{O}_3 + \text{CaO} + \text{Na}_2\text{O} + \text{K}_2\text{O})] \times 100$ (Minyuk et al., 2007; Nesbitt and Young, 1982). The CIA provides the degree and the way these altered rocks are stored on the landscape and transported to the lake; this index also includes a measure of any post-depositional diagenesis. If the source remains constant, it can be interpreted as a proxy for the intensity of chemical weathering. We also use the $\text{K}_2\text{O}/\text{TiO}_2$ ratio as complementary weathering proxy, especially in the periods with high CaO content. K is more concentrated in non-weathered minerals and is leached by weathering processes. Low $\text{K}_2\text{O}/\text{TiO}_2$ ratio occurred during periods of relatively higher terrigenous input due to the soil development in the catchment area (Arnaud et al., 2012).

The *STATISTICA* computer program was used to highlight the correlation of different oxides in order to define the independent variables. Given the variety of proxies used, we also used the same program to unravel the relationship between organic matter geochemistry, grain size, isotopes, and the main independent variables that potentially characterized allochthonous sedimentation (TiO_2 , Al_2O_3 , ZrO_2 , NiO , and Cr_2O_3 ; Table 2).

^{14}C radiocarbon dating (Aeon Radiocarbon Laboratory, US) on 16 samples of terrestrial vegetal remains, shells, ostracods, and micro-charcoals were performed in order to obtain an age model (Table 1). In addition, some age constraint was provided based on the ^{210}Pb and ^{137}Cs radiometric markers measured every 1 cm from the topsoil to 25 cm. Activities of ^{210}Pb and ^{137}Cs were measured using a low-background, high-efficiency, well-shaped γ detector (CANBERRA; Schmidt et al., 2009). Calibration of the γ detector was achieved using certified reference materials (IAEA-RGU-1). Activities are expressed in millibecquerel per gram, and errors are based on 1 SD counting statistics. Excess ^{210}Pb ($^{210}\text{Pb}_{\text{xs}}$) was calculated by subtracting the activity supported by its parent isotope, ^{226}Ra , from the total ^{210}Pb activity in the sediment (Figure 3a).

The age–depth model on the upper part of the core is constrained using ^{210}Pb and ^{137}Cs data (Figure 3). Measured ^{210}Pb values in the upper part of sediment core (18 cm) range from 20 to 11.2 mBq/g (Figure 3a). In general, the downcore distribution of excess ^{210}Pb values follows an exponential decrease with depth. A constant flux:constant rate of supply (CS:CR) sedimentation model was applied (Appleby, 2001). The ^{210}Pb -derived sedimentation rate (SR = 0.46 cm/yr) is slightly thus more important than ^{210}Pb -derived SR corrected with thorium (SR = 0.36 cm/yr). The profile distribution of ^{137}Cs activity shows the maximum at 9 cm depth that represents the period of the maximum 1963 radionuclide fallout. The ^{137}Cs profile is fully compatible with the 0.36 cm/yr thorium-corrected ^{210}Pb -derived SR. This SR implies that the two layers characterized by high MS values and Cr_2O_3 content in the E1 anomalous deposit would correspond to the 1872 and 1822 historical earthquakes (Akyüz et al., 2006; Figure 3a). The two segments of the DSF, the Karasu Fault and the Hacipasa Fault, have ruptured subsequently in 1822 and 1872 in $M \geq 7$ earthquakes (Akyüz et al., 2006). The 1822 earthquake affected most specially the Afrin watershed, disturbing its water flow; Orontes River was also impacted: its course was permanently affected by a landslide (Ambraseys, 1989). The 1872 earthquake ruptured the Hacipasa Fault segment (Akyüz et al.,

2006), lying a few hundred meters from the site and triggered liquefactions near the studied site (Ambraseys, 1989).

The age of the lower part of the core is constrained using radiocarbon dating (Table 1). Dated terrestrial vegetal remains through the core indicate that all vegetal materials are recent and linked to the root system developed by agricultural activities in the dried lake after 1940s. The large depth reached by the deep root system is due to the water table changes between the ground level at the end of the spring to ~10 m at the end of the summer. Regarding shells, the sample age at 78 cm at 2000 ± 20 yr BP implies a reservoir age larger than 1500 years. A similar strong hard-water effect was inferred by Meadows (2005) in the nearby Ghab Basin based on correlation of the pollen diagram of Yasuda et al. (2000) to the Younger Dryas event. The older sample age at 32 cm (2225 ± 25 yr BP) is consistent with the fact that most shells in this level are reworked in relation with the 1872 earthquake. The similar ages of the bivalve shells at 185.5 and 329.5 cm are probably linked to a variable reservoir effect. At the depth of 185.5 cm, CaCO₃ is about ~37%, whereas at the depth of 329.5 cm, it is around ~24%. The hard-water effect is thus probably greater at the shallower depth. The ages of shells are thus very unreliable and cannot be used to constrain an age–depth model. The only reliable materials are micro-charcoals. Micro-charcoals at 398 and 408.5 cm provide calibrated ages of 2755 ± 10 and 2770 ± 11 yr BP, implying that unit 2 was deposited during the Iron

Age. However, the three micro-charcoal samples located above provide ages, about 400–1000 years older, implying large sediment reworking in the watershed. They were excluded from the age model. The other micro-charcoal age at 419.5 cm is 400 years older than the sample located 10 cm above. We infer that the micro-charcoals at this level were also significantly older than their depositional age in the lake. A composite age model was thus built combining the modern ²¹⁰Pb SR, the 1872–1822 earthquake imprints, and the two youngest micro-charcoal ages at 398 and 408.5 cm. The radiocarbon ages imply a significant change in SR. The modern SR was extrapolated to the base of unit 1 at 130 cm depth, where a major change in sedimentation occurred. Below, the grain size decreases sharply, which is coherent with a reduction in SR. Then, we consider a lower and constant SR constrained by the micro-charcoals from 130 cm to the base of the core.

Results

Sedimentological changes recorded based on lithology, grain size and C/N data

The core is mostly composed of brown to gray silty clay with some reddish thin layers with significant macrofossil content (mostly ostracods) near the base. The 4- to 8-cm-thick topsoil, which could not be subsampled at high resolution, is not included in the following log description.

We identify several sedimentary layers characterized by coarse grain particles, a MS higher than the background sedimentation, reworked shells, and/or structural disturbances (plastic deformation and sand pillows). E1, between 20 and 60 cm, is composed of numerous reworked shells and shows two MS increases, one at 34 cm and a larger double peak between 46 and 58 cm. E2 (165–195 cm) is composed of two sandy layers with visible micro-sand pockets and sand dikes probably related to liquefaction. Below, two thin layers at 205 and 225 cm show minor structural disturbances associated with sands. An anomalous event with higher MS and grain size occurred at 260 cm. E3 lies at 330 cm and is characterized by sand pillows in a clay matrix; the typical plastic deformation suggests that the event can be interpreted as earthquake triggered deposit. At 435 cm below a red clay layer, micro-sand dikes suggest another episode of plastic deformation. E4 occurred at 480 cm and shows a 10-cm-thick disturbed sandy layer enriched in shells. E5 at 550 cm is a sand pillow. E6 at the core base (580 cm) is a thick sandy layer rich in plagioclase. All identified events are reported in Figure 4.

Five different sedimentary units were identified (Figure 4) based on the core description, MS, and grain-size data.

Table 1. Calibrated ¹⁴C age results obtained from bivalves, ostracods, and micro-charcoals.

Depth (cm)	Material	¹⁴ C age yr BP ±	¹⁴ C age cal. BP ±
33	Bivalves	2225 ± 25	2246 ± 61
79	Bivalves	2000 ± 20	1956 ± 26
122	Bivalves	2260 ± 25	2267 ± 64
159.5	Wood	<Modern	–
185.5	Bivalves	2820 ± 30	2925 ± 36
221.5	Ostracods	3700 ± 180	4072 ± 250
277	Ostracods	6330 ± 160	7213 ± 179
286.5	Ostracods	6030 ± 280	6886 ± 315
301.5	Micro-charcoal	3615 ± 25	3930 ± 34
318.5	Micro-charcoal	2900 ± 35	3050 ± 62
318.5	Ostracods	3440 ± 150	3720 ± 186
327	Micro-charcoal	3010 ± 25	3219 ± 43
329.5	Bivalves	2820 ± 25	2922 ± 32
398	Micro-charcoal	2620 ± 30	2755 ± 10
408.5	Micro-charcoal	2655 ± 25	2770 ± 11
419.5	Micro-charcoal	3060 ± 35	3288 ± 47

Table 2. Major and minor XRF result correlation, expressed by the coefficient of determination (R^2).

	Na ₂ O (%)	MgO (%)	K ₂ O (%)	CaO (%)	Al ₂ O ₃ (%)	SiO ₂ (%)	TiO ₂ (%)	FeO ₂ (%)	MnO (%)	ZrO ₂ (ppm)	ZnO (ppm)	NiO (ppm)	Cr ₂ O ₃ (ppm)	SrO (ppm)
Na ₂ O (%)	1	-0.1	-0.1	0.1	-0.1	-0.1	-0.1	-0.2	0.1	-0.2	0.0	-0.2	-0.1	0.2
MgO (%)		1	-0.4	0.2	-0.2	-0.1	0.0	0.1	-0.2	-0.2	-0.1	0.6	0.2	0.1
K ₂ O (%)			1	-0.9	0.9	0.8	0.6	0.7	0.3	0.7	0.6	0.0	0.0	-0.7
CaO (%)				1	-0.9	-0.9	-0.7	-0.9	-0.3	-0.7	-0.6	-0.2	-0.1	0.8
Al ₂ O ₃ (%)					1	1.0	0.7	0.9	0.4	0.8	0.6	0.1	0.1	-0.8
SiO ₂ (%)						1	0.7	0.9	0.4	0.7	0.6	0.2	0.1	-0.8
TiO ₂ (%)							1	0.7	0.2	0.7	0.5	0.3	0.1	-0.7
FeO ₂ (%)								1	0.2	0.7	0.5	0.4	0.2	-0.9
MnO (%)									1	0.2	0.2	-0.1	-0.1	-0.2
ZrO ₂ (ppm)										1	0.5	0.1	0.0	-0.7
ZnO (ppm)											1	0.1	0.0	-0.4
NiO (ppm)												1	0.1	-0.2
Cr ₂ O ₃ (ppm)													1	-0.1
SrO (ppm)														1

The bold numbers indicate parameters with a correlation. XRF: x-ray fluorescence.

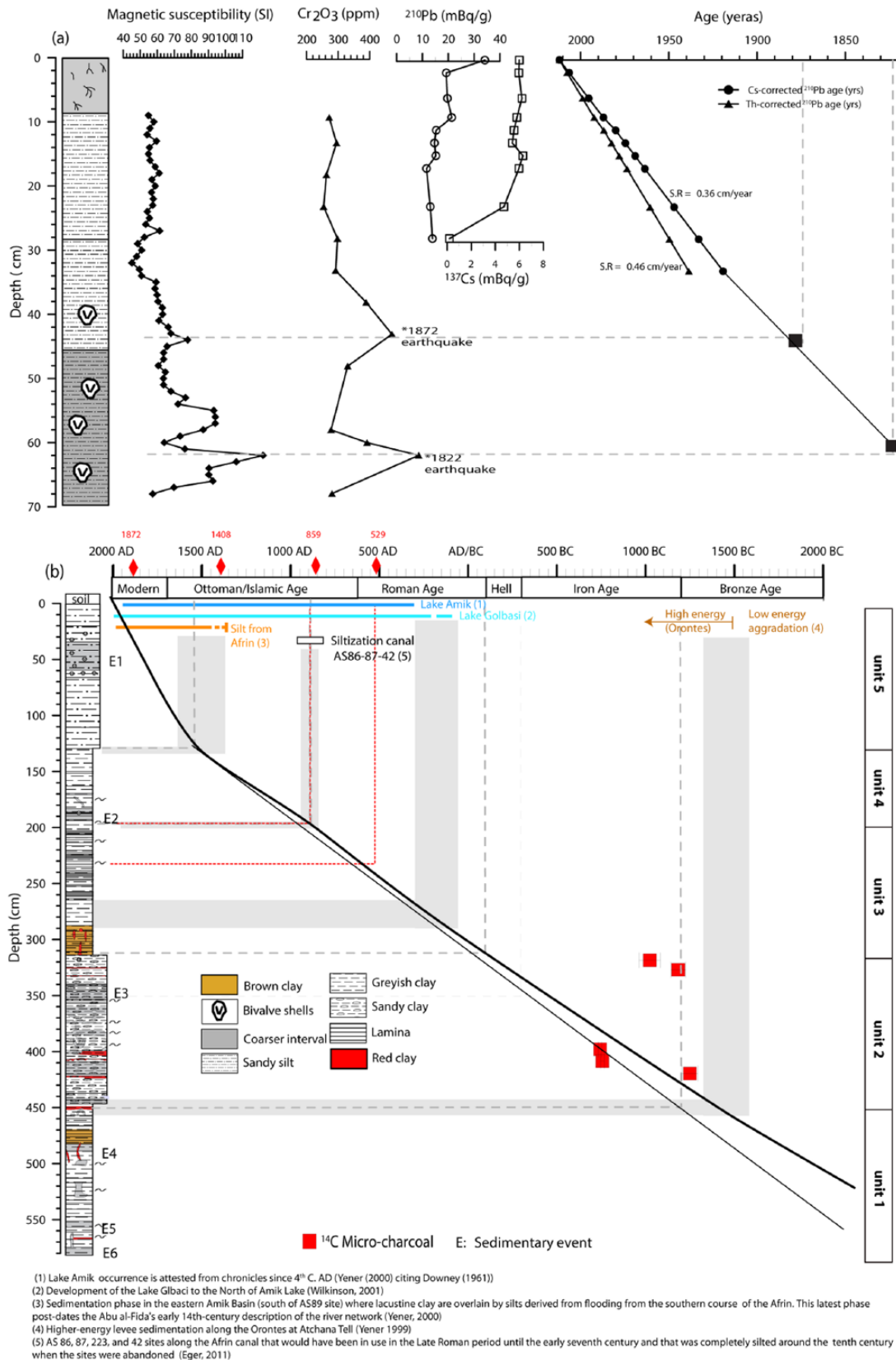


Figure 3. (a) Sedimentation rate and age–depth model from radionuclides (^{137}Cs , ^{228}Th , and ^{210}Pb). The combination of magnetic susceptibility and Cr_2O_3 is used as earthquake tie point to extrapolate the sedimentation rate. (b) Age–depth diagram for Amik Lake based on calibrated ^{14}C age results obtained from micro-charcoal remains, ^{210}Pb and ^{135}Cs activities, correlation with other dated sedimentary sections in the Amik Basin, and historical earthquake tie point (data from Akyüz et al., 2006).

The top unit (unit 5) is 130 cm thick and is characterized by an average MS of 66 ± 16 SI, small variation in C/N, and significant proportion of sand size particles which reach ~80% at 48 cm depth. It is composed of three subunits based on grain-size variation. The 35-cm-thick SU5-3 is characterized by low

values of MS (57 ± 4 SI); sand and silt contents reach 25% and 55%, respectively. Between 20 and 35 cm, eye-visible shells absent in the top part are present and increase in number at the base of the unit. The SU5-2 subunit extends to 60 cm and is the anomalous event with no clay fraction. It shows a large

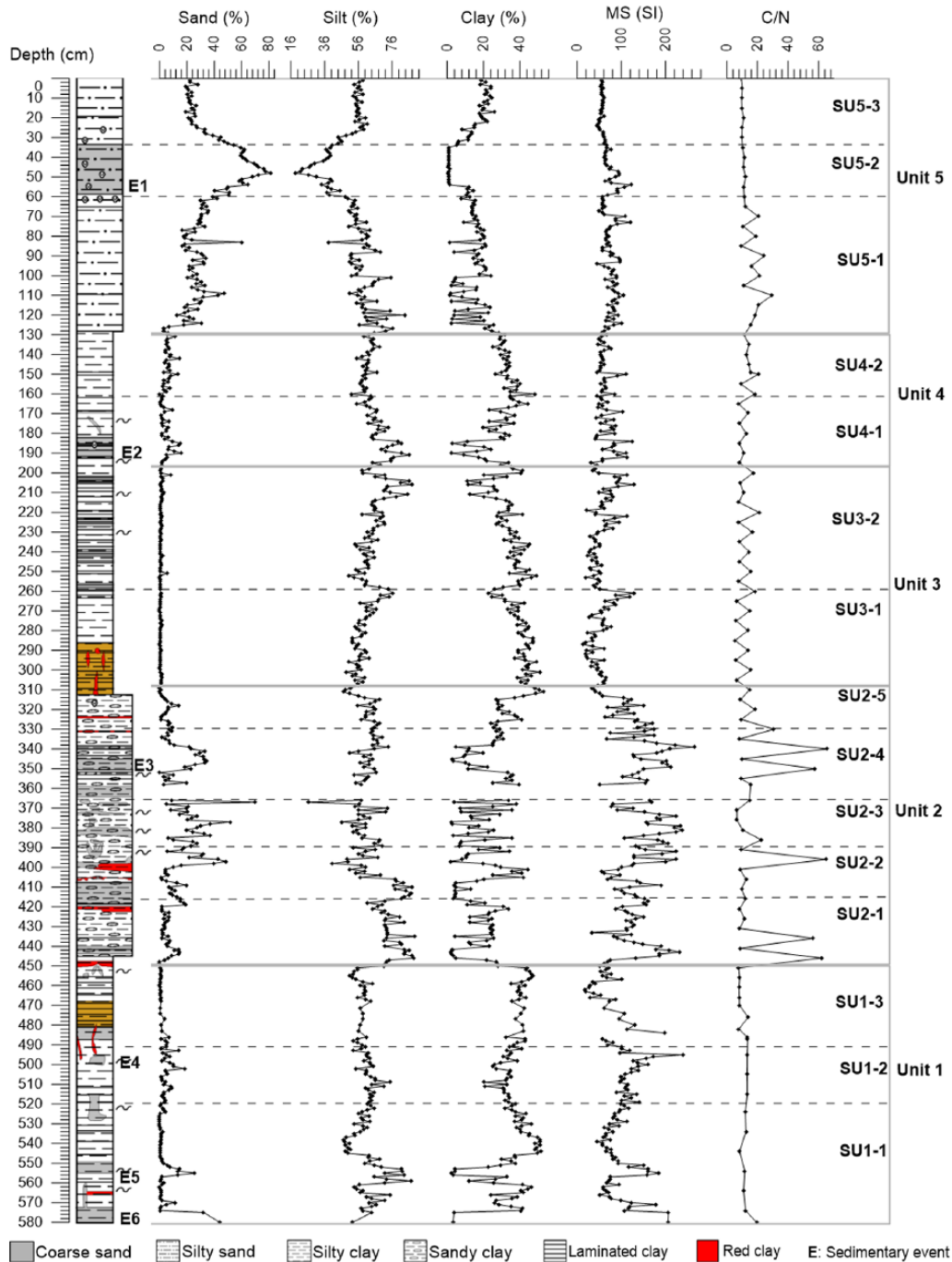


Figure 4. Variations of grain-size distribution (sand, silt, and clay fractions), magnetic susceptibility (MS), and C/N ratio along the depth profile of the Amik Lake.

downward increase in sand size particles comprising reworked shells and in MS peak reaching 120 SI. The silty sand subunit SU5-1 (60–130 cm) has more than 20% of sand fraction, a high macro-organic content, and a high C/N ratio (17 ± 6 , in average). Its sand proportion is composed of a top rich shell layer overlying a sand-rich layer showing a large MS peak reaching 120 SI.

The fourth unit (unit 4) extends from 130 to 196 cm and is mostly silty sand having variable MS values (70 ± 19 SI, in average) and small variation in C/N ratio. Two subunits compose this unit, namely, SU4-1 (196–160 cm) and SU4-2 (160–130 cm), based on the lithology and the grain-size distribution. The SU4-1 is rich in silt than the upper subunit (SU4-2).

The third unit (unit 3) is located between 196 and 308 cm depth below the surface and is characterized by a slightly lower mean MS of 55 ± 25 SI, a low sand content (<5%), and minor

changes in C/N with average values of 14.5 ± 3 . Changes in MS values correspond to changes in the percentage of sand particles (0–15%). Two subunits can be distinguished, SU3-1 (308–260 cm) and SU3-2 (260–196 cm). The SU3-1 subunit shows a basal brownish layer with red nodules that contrasts with its top grayish subunit (SU3-2).

The second unit (unit 2) is located between 308 and 450 cm below the surface and is characterized by coarser grain size ($66 \pm 11\%$ of silt fraction, in average), a higher MS (132 ± 52 , in average), the occurrence of reddish clay levels at the bottom, strong variations in grain size, and very large changes in C/N ratio (20 ± 20 , in average) compared with unit 3 (Figure 4). This unit shows several peaks of C/N with values over 50 corresponding to terrestrial organic-rich layers. Unit 2 can roughly be divided into five subunits: SU2-1 (450–415 cm), SU2-2 (415–390), SU2-3 (390–365 cm), SU2-4 (365–330 cm), and

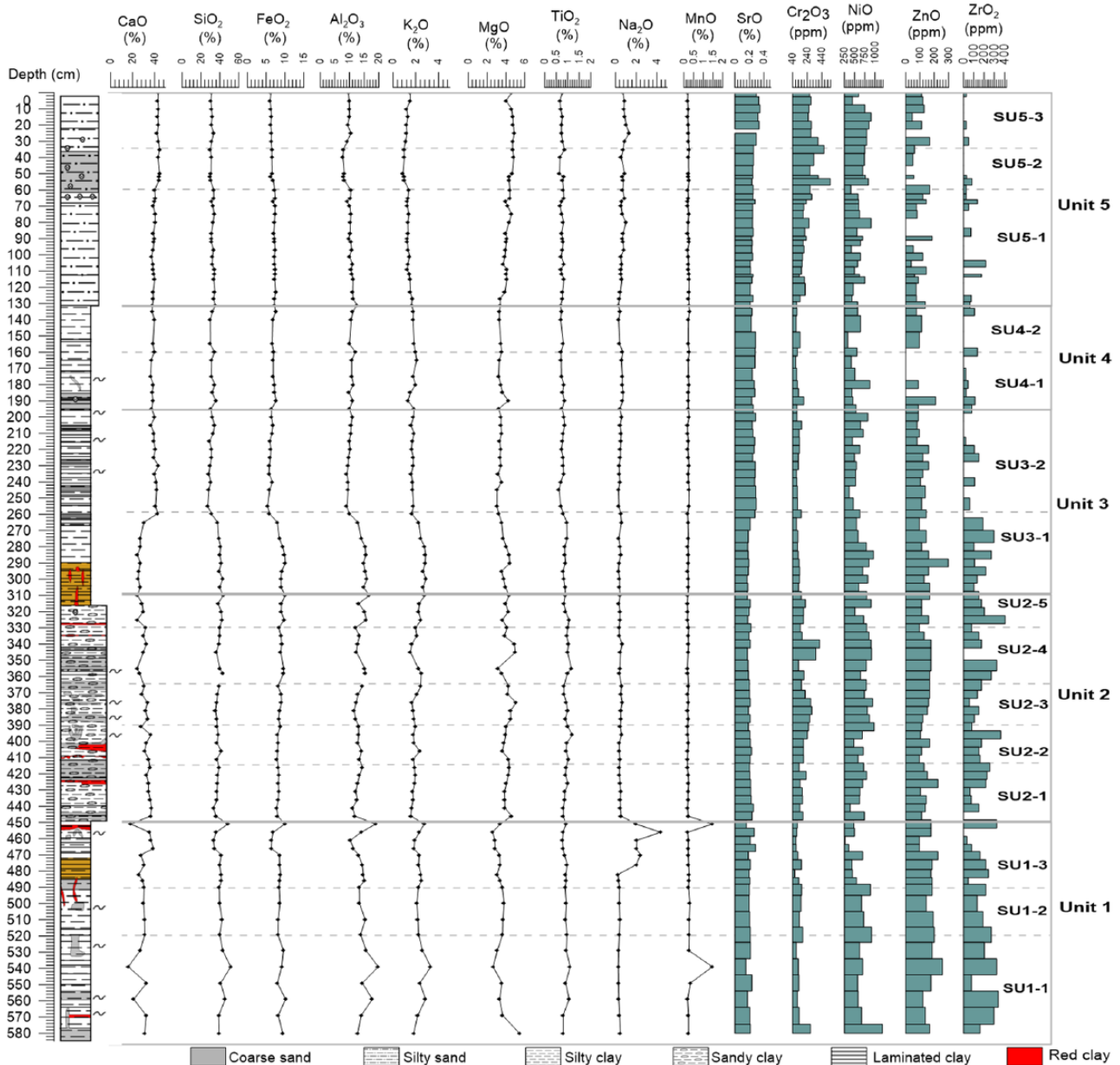


Figure 5. Evolution of major element (oxide form) and minor element (ppm) concentrations along the depth profile of the Amik Lake.

SU2-5 (330–308 cm). The top SU2-5 subunit is a sandy clay in which micro-charcoals were found and dated. The SU2-4 subunit contains several sandy layers without clay and has high MS values. The SU2-3 subunit shows wavy sandy, silty, and clay laminations and sand pillows. The SU2-2 subunit is more homogeneous and fine grained; it is topped by a red clay layer; two dated samples were extracted from this level. The SU2-1 subunit has a sand content particularly low compared with the above unit and contains a basal red clay layer.

The basal unit (unit 1) extends from 450 cm to the bottom of the core and is characterized by high MS values (96 ± 41 SI, in average), low sand content ($4 \pm 6\%$, in average), constant C/N ratio, and the occurrence of reddish clay levels. Three subunits can be deciphered: SU1-3 (450–490 cm), SU1-2 (490–520 cm), and SU1-1 (520–580 cm). The subunit SU1-3 is clayey silt and shows a low MS value compared with the subunits SU1-2 and SU1-1 which are more sandy. SU1-3 basal part has a brownish color, which contrasts the upper grayish part. The SU1-2 is underlined by a marked lithological change; MS and silt show a decrease trend, while clay shows the

opposite pattern. The SU1-1 is characterized by fluctuations in grain size and MS.

Chemical composition (XRF)

The oxides quantified by XRF comprise SiO_2 ($36 \pm 5\%$), CaO ($35 \pm 6\%$), Al_2O_3 ($12 \pm 2\%$), Fe_2O_3 ($8 \pm 1\%$), K_2O ($2 \pm 0.5\%$), TiO_2 ($1 \pm 0.1\%$) as major elements (Figure 5). Most of the CaO is found in calcite, which is the dominant mineral. SiO_2 , K_2O , and Al_2O_3 are incorporated in clays, quartz, plagioclase, and muscovite; Fe_2O_3 is incorporated preferentially in hematite and goethite. K_2O is associated with K-feldspar and clay minerals. In association with calcium, SrO ($0.2 \pm 0.04\%$) is a significant minor element. Large quantities of the following trace elements were found: Cr_2O_3 (160 ± 55 ppm), NiO (654 ± 168 ppm), ZnO (134 ± 49 ppm), and ZrO_2 (155 ± 99 ppm; Figure 5).

The correlation matrix for the oxides (Table 2) provides key information regarding the sedimentation at the site. Most of the major elements (SiO_2 , Al_2O_3 , Fe_2O_3 , and K_2O) are very strongly correlated ($R^2 \geq 0.8$). TiO_2 and ZrO_2 oxides, indicators of soil

erosion, are also strongly correlated to these major elements ($R^2 \geq 0.7$; Table 2). The latter indicates that sedimentation at the site is mostly detrital, related to allochthonous input mostly from the Afrin River, the nearest water source, but also from the Orontes River (Figures 1 and 2). Other oxides such as CaO and SrO are anticorrelated to all the major elements ($R^2 = -0.9$ to -0.7). CaO is weakly correlated to sand size particles and anticorrelated to clay fraction, indicating significant shell fragments, and would thus represent the lake productivity. Cr_2O_3 and NiO are independent oxides.

The chemical composition significantly changes with increasing depth of the core. The upper unit (unit 5) contains $42 \pm 2\%$ of CaO, $32 \pm 1\%$ of SiO_2 , $10 \pm 1\%$ of Al_2O_3 , and $7 \pm 0.5\%$ of Fe_2O_3 . Trace elements show the prevalence of NiO (652 ± 144 ppm) and Cr_2O_3 (225 ± 100 ppm), whereas ZrO_2 is particularly low (35 ± 55 ppm). The geochemical fingerprint of SU5-2 is particularly well defined marked by a very high CaO content related to the occurrence of numerous reworked shells in the layer and high SiO_2 and Fe_2O_3 percentage probably related to the concomitant decreases in clay size particle. It also shows two Cr_2O_3 peaks comprising the largest percentage recorded in the whole core. NiO values increase in parallel to Cr_2O_3 in unit 5.

Unit 4 is characterized by large amount of CaO ($38 \pm 1\%$) and SiO_2 ($33 \pm 1.7\%$). Small amounts of Fe_2O_3 ($7 \pm 0.4\%$), Al_2O_3 ($11 \pm 0.7\%$), and K_2O ($2 \pm 0.3\%$) compose this unit. This decrease in iron associated with an increase in CaO will suggest anoxic conditions. Trace elements show the prevalence of NiO (535 ± 151 ppm) and Cr_2O_3 (115 ± 33 ppm), whereas ZrO_2 is low (52 ± 52 ppm).

Within unit 3, a major and sudden change occurred at 255 cm between subunits SU3-1 and SU3-2: most of the major elements suddenly increase downward, while CaO and SrO amount shows the opposite trend. CaO decreases from $40 \pm 2\%$ to $28 \pm 5\%$, and SiO_2 , Al_2O_3 , and Fe_2O_3 jump, respectively, from $30 \pm 2\%$ to $39 \pm 4\%$, $10 \pm 1\%$ to $15 \pm 2\%$, and 6 to 9% . Trace elements ZnO, ZrO_2 , and NiO also increase downward, respectively, from 89 ± 49 to 174 ± 74 ppm and 570 ± 127 to 731 ± 138 ppm, while Cr_2O_3 remains constant around 123 ± 20 ppm.

In units 2 and 1 (308–580 cm), CaO increases slightly to $31 \pm 4\%$, while K_2O decreases compared to the above unit. Cr_2O_3 increases to 188 ± 46 ppm and ZrO_2 content reached its maximum in this unit. A marked geochemical signature characterized by punctual increase in Al_2O_3 , SiO_2 , TiO_2 , and K_2O and a very large Cr_2O_3 peak indicates a sedimentary event. Trace elements such as ZrO_2 , NiO, and Cr_2O_3 are slightly lower in the subunit SU1-3.

Age–depth model and SR

We independently correlated our sedimentary cores with other dated sedimentary sections in the Amik Basin and took into account textural evidences. We focus on studied sites close to our coring site, in the eastern part of the Amik Basin, but we also consider major recorded environmental changes that would influence sedimentation at the coring location (see Figure 2). The timing of most these environmental changes was constrained within the framework of archaeological investigations (i.e. Yener et al., 2000) and is based on change in pottery styles and artifacts.

The largest environmental change, which rests on the largest body of evidences, is the large growth of a lacustrine body during the Roman/early Islamic time, which triggered an inundation of cultivated soils, the abandonment of settlements, and their shift to the outer margin of the basin (see Figures 2 and 3). The occurrence of a lake is attested in chronicles since the 4th century (Yener et al., 2000, citing Downey, 1961). The border of the lake during the Roman and late Roman Periods is attested by the sand ridge on the eastern side of the lake containing potteries from that time (Eger, 2011). A lake-level increase above this ridge is attested at sites AS 86 and AS 87 to the east and in section along the Afrin drain. The inundated cultivated lands (brown clay soils)

were covered by grayish lacustrine clay. The same lake-level increase is recorded at site AS 180, which became an island during the Roman Period (Wilkinson, 2000). The lake-level increase first affected sites in the inner part of the basin and to the east and then it affected sites to the north. Sites AS 187, 32, 29, and 28 were abandoned because of flooding before the end of the 13th century (Yener et al., 2000). This large environmental change matches in our sedimentary record the change between the sandy unit 2 and the clayed unit 3 (see Figure 3b).

Three other environmental changes could have impacted the coring site. First, the Afrin canal very close to the coring site was likely completely silted by 10th century, and sites AS 86, 87, 223, and 42 along the canal occupied during the 7th century were abandoned by 10th century (Figure 2; Eger, 2011). The change in water supply would directly affect the sedimentation at the coring site and would correspond to the transition between the clayey unit 3 and the sandy clay unit 4. The second one occurred during the Ottoman/Islamic Period, again, along the Afrin River in the eastern part of the basin. Silty clay derived from the Afrin River overlies the lacustrine clay deposited since the end of the late Roman Period (Figure 3, south of site AS 89). These coarser grained deposits were related to a southward shift of the Afrin River that would have occurred after the travel of Abu-al Fida at the beginning of the 14th century in the region (Yener et al., 2000). We correlated this change with the strong increase in grain size observed between unit 4 and unit 3. The last environmental change is related to the Orontes, the largest river supplying water to the Amik Basin. The drain of the Bronze Age Tell Atchana evidenced a strong change in activity along the Orontes from a low-energy aggradation to high-energy flooding (Yener et al., 2000). This environmental change would correspond to the large increase in grain size from clayed unit 1 to sandy unit 2.

As a final test regarding the age model, we compare the inferred ages of the sedimentary events with historical earthquakes in 1872, 1408, 859, and 525 that would have ruptured the Hacipasa Segment (Akyüz et al., 2006; Meghraoui et al., 2003; Yönlü et al., 2010). The main sedimentary event E2 would correspond to the 859 event, the 525 earthquake to a minor sedimentary event below, and the 1408 event would not be recorded. The events that could reflect the seismic history are compatible with the age model.

Although the ^{14}C age model is impressive, the independent correlation of the sedimentary core with the recorded environmental changes validates it. We considered that the sediment deposited through unit 1 corresponds to the late Bronze Age (2000–1200 BC), unit 2 corresponds to the sediments deposited throughout the Iron Age (1200–300 BC) and Hellenistic Period (300–100 BC), unit 3 was deposited during the Roman and early Islamic Periods (100 BC–AD 650), unit 4 comprises the sediments from the Islamic and Ottoman Periods (AD 650–1650), and unit 1 represents the Modern Period.

Interpretation

Our record of the beginning of the late Bronze Age (~2500 BC) reveals continuous lacustrine or marshy environments with short or seasonal emersion. This interpretation is still compatible with previous insights based on a core and settlements in the central and southern part of the lake (Casana, 2014; Wilkinson, 2000). Tell sites AS 180 and AS181 were small farms around the late 3rd-century BC (Casana, 2014; Eger, 2008), so the lake was inferred to be very small or inexistent at that time. The fact that a lake prevailed at our coring site is due to the specific coring location near the northern extremity of the Hacipasa Fault segment, where a significant normal component is expected. Tectonic subsidence at our coring location is larger than in the central or southern part of the lake; as a consequence, a restricted water

body prevailed at the studied location even though it was absent in others.

Different environments and marked changes are recorded and summarized below from the oldest to the younger one.

During the Bronze Age (unit 1), the clayey fine-grained sediments with ostracod shells attest the occurrence of a low-energy lacustrine environment with little external input. Wilkinson (2005) and Yener (2005) affirmed that the fluvial environment of the early/middle Holocene in the Amik plain was relatively stable. The occurrence of brownish sediments with ostracods suggests a seasonal reduction in the water column (oxic environment) probably during summer months when the evapotranspiration is the highest. The subsequently deposited grayish clay sediments imply a renewed deepening of the water depth. These two clay types were used for the bricks of the nearby Bronze Age Karatepe Tell (AS 86; Yener, 2000). The high ZrO_2 , Cr_2O_3 , and ZnO content attests the occurrence of active soil erosion in the Amanus Mountains.

A first major environmental change occurs at the transition between the late Bronze and Iron Ages. The latter is characterized by the anomalous clayey subunit SU1-3 with a high percentage of NaO and CaO and low FeO - MgO , which suggests oxic conditions with a very low water level. The upward decrease in ZrO suggests a drastic reduction in soil erosion related to aridification and/or to decreased anthropic pressure. The top subunit is marked by a sedimentary event probably related to an earthquake. During the Bronze/Iron transition, the main regional center Tell Atchana was abandoned, and Tell Ta'yinat, located 400 m more to the east, was reoccupied (Welton, 2012). The subunit is capped by a 3-mm red clay layer suggesting oxic conditions probably with temporary emersion and overlain by the sandy subunit SU2-1, in which high C/N ratio indicates terrestrial organic matter. This environmental context suggests the occurrence of a drought. An aridification during the late Bronze/early Iron Age transition was repeatedly documented in the Eastern Mediterranean and it was associated with the collapse of the Hittite civilization (end of the 13th-century BC; e.g. Kaniewski et al., 2015; Weiss, 1982). Although we document a clear major sedimentary change between the late Bronze and Iron Ages, there was no apparent societal collapse in the Amik Basin. There was a decline in settlements during the late Bronze Age, but in the Iron Age new settlements appeared and then concentrated in the southern part around the Tell Ta'yinat (Casana, 2007). The trade pattern was disrupted at the Bronze/Iron transition (Janeway, 2008), but farming increased at that time (Capper, 2012). Although a more arid environment is attested by our study, the Amik Basin was still a rich fertile land that allowed a sustainable growth of the agricultural societies in this area (Casana, 2007).

During the Iron Age, the high percentage of sand and high C/N ratio attest for the occurrence of a drier climate with a low lake level and the colonization of a terrestrial vegetation near the coring site (Figure 4). Part of this period corresponds to the arid Dark Age Period identified in Gibala-Tell (Tweini) along the Syrian coastline, at about 100 km from our site (Kaniewski et al., 2008). The variable and rapidly changing grain size of the subunits implies a high-energy environment compared with the lower unit 1. The high content in Cr_2O_3 , ZrO_2 , and NiO (Figure 5) points to an ongoing soil erosion in the Amik watershed and could indicate a starting occupation of the highlands and an increased deforestation phase related to the extension of the agricultural activities such as orchards. After the Iron Period, during the Hellenistic Period, the Amik plain was densely occupied and sites in the highland started to be occupied (Gerritsen et al., 2008).

The Roman and early Islamic Periods (unit 3) were associated with the development of the Antioch city and the complete intensive occupation of the highlands. The sediments during this period are clays devoid of sands, with low MS and minimal variability implying a low-energy environment. The low C/N values indicated

a low input of terrestrial organic matter. The very low terrigenous inputs during the Roman/early Islamic Periods are also attested by the low MS values during this period. Aggradation at the Judaidah and Qarqur sites (Figure 2) was an order of magnitude lower than during the Bronze/Iron Period. However, the occurrence of high colluvium thickness in the Jebel-al-Aqra low range in the late Roman Period suggests a high soil erosion episode in the Amik watershed. However, a significant portion of the sediments eroded at this time was stored locally as colluviums within the ranges by terraced terrains, in agreement with the absence of soil erosion indicators at our site, and did not reach the lake. The Roman Period (subunit SU3-1) shows some difference with the early Islamic Period (subunit SU3-2). The ZrO_2 decreased sharply and would never rise again significantly suggesting a permanent fall of soil erosion at the end of the Roman Period, possibly related to a permanent removal of the mobile soil cover on sensitive areas. The transition is also characterized by an abrupt increase in CaO and a concomitant small decrease in terrigenous elements by dilution. The increase is not associated with a significant change in grain size, organic matter, and any major biological activity. This carbonate increase must be related to an increase in $CaCO_3$ in water provided by the Afrin River associated with the canal construction and exploitation near our site (Yener, 2000). Finally, the transition and the above SU3-2 unit are marked by small sedimentary events. The period was marked by a cluster of seismicity with major earthquakes from the 6th- to the 9th-century AD (Akyüz et al., 2006). Among them, the AD 859 and 525 earthquake ruptured the Hacıpasa Fault that is adjacent to our site.

During the Ottoman/Islamic Period (unit 4), the sediments deposited show an increase in the clay fraction and a fall in ZnO amount. During the Islamic Period, 50% of the settlements disappeared (Eger, 2015). The clayey sediments is attested by a very low-energy and a lacustrine environment. The small increase in grain size between units 3 and 4 may be related to changes in water inflow from the different canals of the Afrin River, in which distribution changes through time (Figure 1). Siltization of the canal near our site may have occurred (Eger, 2015), but the canal branch B more to the north passing through Aktas was built and functioning at that time (Figure 2).

The Modern Period (unit 5) starting during the 17th century is characterized by an increase in coarse particles and higher C/N ratio, suggesting an increase in terrigenous sediments with terrestrial organic matter (Figure 4). The Cr_2O_3 , ZnO , and NiO contents increase slightly and support a renewed exploitation from the ophiolitic Amanus terrains. Enhanced erosion was caused, in particular, by the construction of the first railway line in Turkey since 1856 under the Ottoman Empire, first by a British and then by the German and French companies for both economic and strategic reasons, due to the important position of the region in the trade between Europe and Asia (Zurcher, 2004). In recent years, to increase the amount of croplands for food production, the Amik Lake was progressively dried starting as early as 1940. In 1965, about 6700 ha of the Amik Lake and 6800 ha of its surrounding wetlands were drained (International Engineering Company (IEC), 1966). Since 1965, croplands and settlements increased until a complete drying of the lake in 1970. A significant part of the former Amik Lake flooded during Spring time. The progressive drying is attested by an increase in CaO and a decrease in FeO_2 (oxidation).

Discussion

Geochemical and sedimentological analyses of the sediments indicate that the landscape of the Amik plain has drastically changed over the last 4 kyr in relation with land-use and human occupation phases. In this section, the CIA index and K_2O/TiO_2 , Cr_2O_3/NiO , and Cr_2O_3/Zr_2O ratios are used as climatic and erosion proxies to further discuss land degradation.

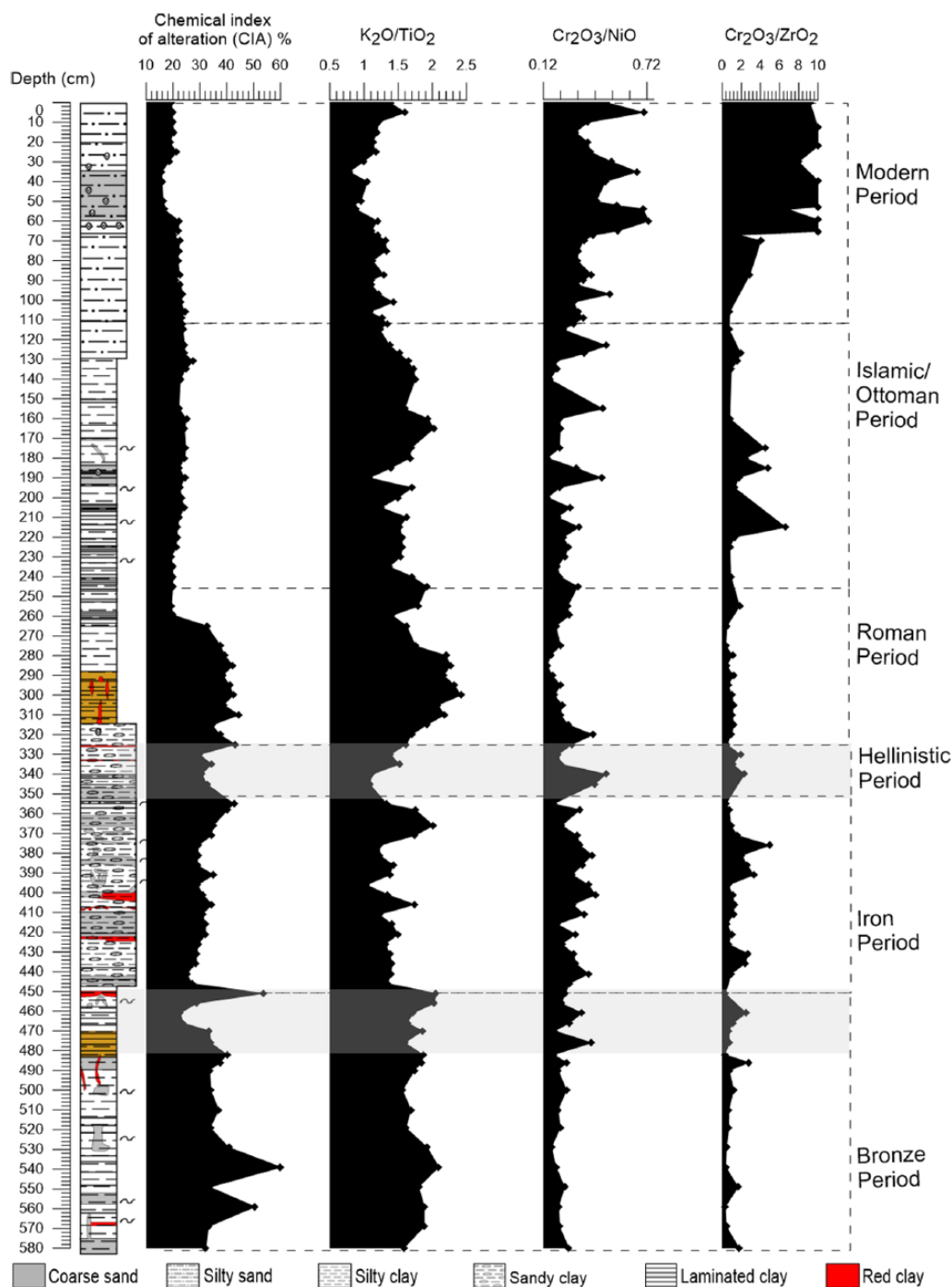


Figure 6. Variations of CIA, physical weathering (K_2O/TiO_2), and C_2O_3/TiO_2 and C_2O_3/ZrO_2 ratios along the archaeological periods in the Amik plain. Gray area indicates intervals of low chemical weathering phase.

In the late Bronze and Iron Ages, soil erosion occurred in association with the development of numerous settlements attested by high terrigenous content, MS, and ZrO_2 content. The land degradation was intense particularly during the Iron Period affecting also the highland. The documented land degradation and the associated soil erosion resulted in widespread aggradation documented at two major settlements in the Amik Basin, Tell Judaidah where aggradation reached 12 m/kyr during the Bronze Age and Tell Atchana where an even higher aggradation rate of ~17 m/kyr was observed (Casana, 2012). By comparison, the aggradation rate at Tell Judaidah during the late Chalcolithic was an order of magnitude smaller, which confirms the high erosion rate on the hillslopes and ranges surrounding the Amik plain starting in the Bronze Age. During this period, agrarian and pastoral sector developed remarkably with the use of plowing and the cultivation

of fruit-tree, and the agricultural lands in the Amik region were probably the most fertile low lands and the bottom of some valleys in proximity with the tell settlements (Akkermans and Schwartz, 2003; Yener, 2005).

In addition, an intense deforestation would have prevailed on the Amanus Mountains exploiting cedars (Rich, 2013; Rowton, 1967). Timber harvesting was a primary economic interest at that time, and forests were heavily exploited during the Bronze and Iron Ages (Rich, 2013). The Amanus Mountains were the prime location for the cedars used in Mesopotamia (Hansman, 1976). Its deforestation is confirmed in our record by the high amount of chromium, zinc, and nickel, as specific markers of the ophiolites outcropping there. There is small difference between the Iron and the Bronze Ages. During the Bronze Age, nearly steady erosion occurred except at the end of the Bronze Age, whereas during the

Iron Period, the highly variable grain size, Zr_2O content, and MS suggest episodic erosion. Additional factors triggering soil erosion from the Amanus Mountains would be the clearing of a route across mountains between the Amik and Cilicia Plain west as well as the exploitation of metals and minerals. The Amanus Mountains had natural gold, chromite, copper, and arsenic resources (Yener et al., 2000). Cr_2O_3/ZrO_2 ratio shows a small increase during the Iron Age, suggesting chromite exploitation possibly for faience glazes (Groot et al., 2006; Figure 6), and Cr_2O_3 content was maximal during the late Iron Period, suggesting a combination of deforestation, road clearing, and ore exploitation in full agreement with the documented human occupation history (e.g. Welton, 2012).

The late Bronze Age collapse period is particularly visible in the CIA index. The low CIA corresponds to the input of less weathered sediments in the lake and indicates a runoff of low intensity and a low residence time for sediments in transport to the lake (Minyuk et al., 2007). The low CIA during the early Iron Age called the Dark Age suggests that the dry conditions that occurred during the late Bronze Age collapse period have continued during the Iron Dark Ages. A dry Iron Age was also documented in the low lake levels of the Dead Sea (Frumkin and Elitzur, 2002).

The Roman Period is marked by canal constructions, which completely changed the sedimentation pattern at the investigated site. The CIA and K_2O/TiO_2 are very high and indicated erosion of already well-weathered materials to the lake. The low grain size and MS imply that the coarsest part of this terrigenous input was trapped upstream in agricultural terraces and in the Afrin canals. During the Roman Period, an intensive agricultural occupation started on the calcareous plateau to the south of the Amik Basin and along the Orontes River upstream the Amik Lake, which created the necessary preconditions for severe soil erosion to occur (Casana, 2008). This phase of severe soil erosion occurred resulting in the deposition of 3.5–5.0 m of alluvial sediments on valley floors in several small drainage basins in the Jebel al-Aqra region (Casana, 2008) to the south of the Amik Basin (Figures 1 and 2). The high K_2O/TiO_2 during the early part of the Roman Period might be linked to the Roman Climatic Optimum, which was responsible for high water levels in the Dead Sea (Bookman et al., 2004). At the end of the Roman Period and beginning of the Islamic Period, the strong decrease in ZrO_2 content associated with the fall in CIA, the decrease in K_2O/TiO_2 , and the sudden rise in CaO content imply a major change in the watershed. We suggest the following scenario. When the thin soil organic covered was stripped from the calcareous highlands, there was a more direct contact between rainfall and the bared calcareous reliefs, which increased the diluted CaO content in the Amik watershed and resulted in a higher Ca deposition in the Amik Lake. The soil removal would have tremendously decreased the crop production on these uplands. In the Orontes watershed, on the limestone uplands of western Syria, villages and farmsteads were abandoned at the end of the 7th century forming the Dead Cities (Tchalenko, 1953). The soil removal also resulted in a drastic reduction in the chemical alteration of these ranges, which triggered a decreased production of terrigenous materials and ZrO_2 . The fact that ZrO_2 and MS were low even during the Modern Period is consistent with the proposed interpretation of soil depletion and the fact that a large fraction of the mature soil was removed in the Amik watershed at the end of the Roman Period. This process did not affect the ophiolitic Amanus Mountains, as Cr_2O_3 , NiO, and ZnO contents did not show a similar decrease. The early Islamic Period is also characterized by a fall in population and occupation, which resulted in a decreased anthropic pressure. About 50% of the settlements disappeared (Eger, 2011), and the population of Antioch sharply decreased during the 7th century due in particular to natural hazard (mainly plague and

earthquakes). There was also a complete change in agricultural practice with agriculture practiced only in localized fields and a strong development of nomadic pastoralism in relation with an increase in mashification of the Amik plain and its fertile land (Gerritsen et al., 2008; Wilkinson, 1998).

The Islamic Period is characterized by an upward increase and then a decrease in K_2O/TiO_2 ratio. The optimum around AD 1250 might correspond to the 'Medieval Warm Period (Kaniewski et al., 2011). The decline of the region increased with a widespread nomadic pastoralism, but some wheat, olive trees, vines, fruit-bearing trees were still exploited (Gerritsen et al., 2008; Sorrel and Mathis, 2016). The enhanced pastoralism and the unmaintained terraced terrains in the highlands have renewed soil erosion. In Mediterranean landscapes, unprotected soils under pastures are thinner and more erodible than soil occupied by olive trees with terracing (Marathianou et al., 2000).

The Modern Period is characterized by an increase in anthropic pressure with the development of an intensive agriculture associated with the drying of the lake and a renewed development of the Antioch/Antakya city. The ZrO_2 content remains very small confirming the permanent decrease in soil erosion in probably the calcareous part of the watershed. Cr_2O_3 and NiO increased significantly compared with the previous period, implying a renewed degradation of the Amanus Mountains triggered by road construction, ore exploitation, and deforestation.

Conclusion

Sedimentological and geochemical analyses highlight large environmental changes in the Amik Lake during the last 4 kyr and the potential influence of human occupation on the landscape, especially the erodible and sensitive highlands. Several erosion phases were documented and discussed in the light of the archaeological settlement history and climate fluctuations and partly to the increase in human settlements. The major trends in terrigenous inflow to the lake were also presented.

Anthropic pressure on the highland is already strong in the late Bronze Age characterized by a strong aggradation period linked to soil erosion with specific characteristics: high MS values and percentages in ZrO_2 , NiO, Cr_2O_3 , and ZnO. The climatic degradation at the Bronze/Iron transition is identified and presents a major crisis, which apparently did not significantly disrupt the human occupation through soil erosion that was greatly reduced at that time implying a decrease in the anthropic pressure on the landscape. The Iron Age was at the beginning arid with strong climatic fluctuation and a high anthropic pressure on the landscape characterized by coarse grain size; very high MS values; high amount of ZrO_2 , NiO, Cr_2O_3 , and ZnO; and a supply of organic matter of terrestrial origin. Landscape sustained a strong deforestation, which leads to large upland cultivation and orchard starting in the Hellenistic Period. The Roman Period was characterized by a large environmental change near the coring site linked to channeling of the water of the different rivers and to the progressive increase in water level of the lake. Only fine-grained clay material reached the site, but high ZrO_2 , ZnO, NiO, and CIA content implies ongoing soil erosion. The coarsest materials were probably stored in the highland in terraced terrain or in the canals. The early Islamic period attests for a permanent and strong change in the watershed marked by a permanent decrease in ZrO_2 and MS and increase in CaO. The change would be linked to the stripping of the thin soil covers from the limestone upland, which triggered a hardening of the water and a decrease in the chemical weathering of the limestone upland. During the Islamic/Ottoman Period, the sharp decrease in population did not trigger a significant landscape restoration. Silty clay deposited with a larger MS than during the early Islamic Period suggests that the prevailing pastoralism on sensible highlands without preserved terracing is not a

favorable practice regarding soil erosion in agreement with the previous study on the Mediterranean landscape. During the Modern Period, the more intensive human occupation triggered an increase in Cr₂O₃ and NiO related to the enhanced soils erosion from the Amanus Mountains, linked to large-scale deforestation and ore exploitation. The low ZrO₂ and MS values compared with the Iron/Bronze/Roman Periods imply a permanent decrease in erosion that we related to the stripping of the soil cover during this period on the calcareous highlands.

Funding

The author(s) received no financial support for the research, authorship, and/or publication of this article.

References

- Akkermans PM and Schwartz GM (ed.) (2003) *The Archaeology of Syria: From Complex Hunter-gatherers to Early Urban Societies (C. 16,000–300 BC)*. Cambridge: Cambridge University Press.
- Akyüz HS, Altunel E, Karabacak V et al. (2006) Historical earthquake activity of the northern part of the Dead Sea Fault Zone, southern Turkey. *Tectonophysics* 426: 281–293.
- Altunel E, Meghraoui M, Karabacak V et al. (2009) Archaeological sites (tell and road) offset by the Dead Sea Fault in the Amik Basin, southern Turkey. *Geophysical Journal International* 179: 1313–1329.
- Ambraseys NN (1989) Temporary seismic quiescence: SE Turkey. *Geophysical Journal International* 96(2): 311–331.
- Appleby P (ed.) (2001) *Chronostratigraphic Techniques in Recent Sediments, Tracking Environmental Change Using Lake Sediments*. Dordrecht: Springer.
- Arnaud F, Révillon S, Debret M et al. (2012) Lake Bourget regional erosion patterns reconstruction reveals Holocene NW European Alps soil evolution and paleohydrology. *Quaternary Science Reviews* 51: 81–92.
- Batiuk SD (2005) *Migration theory and the distribution of the Early Transcaucasian Culture*. PhD Thesis, University of Toronto.
- Bookman R, Enzel Y, Agnon A et al. (2004) Late-Holocene Lake levels of the Dead Sea. *Geological Society of America Bulletin* 116(5–6): 555–571.
- Boulton SJ, Robertson A HF, Ellam RM et al. (2007) Strontium isotopic and micropalaeontological dating used to help redefine the stratigraphy of the Neotectonic Hatay Graben, southern Turkey. *Turkish Journal of Earth Sciences* 16: 1–39.
- Braidwood RJ and Braidwood L (1960) *Excavations in the Plain of Antioch I: The Earlier Assemblages, Phases A–J* (Oriental Institute Publication). Chicago, IL: Oriental Institute Press.
- Braidwood RJ, Çambel H and Schirmer W (1981) Beginnings of village-farming communities in Southeastern Turkey: Cayönü Tepesi, 1978 and 1979. *Journal of Field Archaeology* 8: 249–258.
- Butzer KW (2005) Environmental history in the Mediterranean world: Cross-disciplinary investigation of cause-and-effect for degradation and soil erosion. *Journal of Archaeological Science* 32: 1773–1800.
- Çalışkan V (2008) Human-induced wetland degradation: A case study of Lake Amik (southern Turkey). In: *Third international conference on water observation and information system for decision support* (Balwois), Ohrid, 27–31 May 2008.
- Capper MM (2012) *Urban subsistence in the Bronze and Iron Ages: The palaeoethnobotany of Tell Tayinat, Turkey*. PhD Thesis, Department of Archaeology.
- Casana J (2003) *From Alalakh to Antioch: Settlement, land use, and environmental change in the Amuq Valley of southern Turkey*. PhD Thesis, Department of Near Eastern Languages and Civilizations, University of Chicago.
- Casana J (2007) Structural transformations in settlement systems of the northern Levant. *American Journal of Archaeology* 111: 195–221.
- Casana J (2008) Mediterranean valleys revisited: Linking soil erosion, land use and climate variability in the Northern Levant. *Geomorphology* 101: 429–442.
- Casana J (2012) 7 settlements, territory, and the political landscape of late bronze age polities in the Northern Levant. *Archeological Papers of the American Anthropological Association* 22: 107–125.
- Casana J (2014) The late Roman landscape of the Northern Levant: A view from Tell Qarqur and the lower Orontes River Valley. *Oxford Journal of Archaeology* 33: 193–219.
- Casana J and Wilkinson TJ (2005) Settlement and landscapes in the Amuq region. *Amuq Valley Regional Projects* 1: 1995–2002.
- De Giorgi AU (2007) The formation of a Roman landscape: The case of Antioch. *Journal of Roman Archaeology* 20: 283–298.
- Doğruel F and Leman J (2009) Conduct and counter-conduction the Southern border of Turkey: Multicultural Antakya. *Middle Eastern Studies* 45: 593–610.
- Downey A (1961) *A History of Antioch in Syria: From Seleucus to the Arab Conquest*. Princeton, NJ: Princeton University Press.
- Dunjo G, Pardini G and Gispert M (2003) Land use change effects on abandoned terraced soils in a Mediterranean catchment, NE Spain. *Catena* 52: 23–37.
- Eger A (2008) *Settlement and landscape transformations in the Amuq Valley, Hatay: A long-term perspective*. PhD Thesis, The University of North Carolina at Greensboro.
- Eger A (2011) The swamps of home: Marsh formation and settlement in the early medieval near east. *Journal of Near Eastern Studies* 70: 55–79.
- Eger A (ed.) (2015) *The Islamic-byzantine Frontier: Interaction and Exchange among Muslim and Christian Communities*. New York: I.B. Tauris.
- Friedman I, Trembour FW and Hughes RE (1997) Obsidian hydration dating, in Chronometric dating in archaeology. In: Taylor RE and Aitken MJ (eds) *Advances in Archaeological and Museum Science 2*. New York: Springer/Plenum Press, pp. 297–321.
- Frumkin A and Elitzur Y (2002) Historic Dead Sea level fluctuations calibrated with geological and archaeological evidence. *Quaternary Research* 57(3): 334–342.
- Gerritsen F, De Giorgi A, Eger A et al. (2008) Settlement and landscape transformations in the Amuq Valley, Hatay: A long-term perspective. *Anatolica* 34: 241–314.
- Groot NCF, Dik J, Van der Kooij G et al. (2006) Dark and shiny: The discovery of chromite in Bronze Age faience. *Archaeometry* 48(2): 229–236.
- Grove A (1996) The historical context: Before 1850. In: Brandt CJ and Thornes JB (eds) *Mediterranean desertification and land use*. Chichester: Wiley, pp. 13–28.
- Gülen L, Barka A and Toksöz MN (1987) Continental collision and related complex deformation: Maras triple junction and surrounding structures, SE Turkey. *Hacettepe University Earth Science Journal* 14: 319–336.
- Haines RC (1971) *Excavations in the Plain of Antioch II: The Structural Remains of the Later Phases. Chatal Hüyük, Tell Al-judaidah, and Tell Ta'yinat*. Chicago, IL: Oriental Institute Press, pp. 92.
- Hansman J (1976) Gilgamesh, Humbaba and the land of the ERIN-trees. *Iraq* 38(1): 23–35.

- International Engineering Company (IEC) (1966) *Technical and Feasibility Report of Amik Development: Projects of Lake Amik and Tahtaköprü Dam*. Ankara: Ministry of Energy and Natural Resources, State Hydraulic Works.
- Janeway B (2008) The nature and extent of Aegean contact at Tell Ta'ayinat and vicinity in the Early Iron Age: Evidence of the sea peoples? *Scripta Mediterranea* 27: 123–146.
- Kaniewski D, Guiot J and Van Campo E (2015) Drought and societal collapse 3200 years ago in the Eastern Mediterranean: A review. *Wiley Interdisciplinary Reviews: Climate Change* 6: 369–382.
- Kaniewski D, Paulissen E, Van Campo E et al. (2008) Middle East coastal ecosystem response to Middle-to-Late-Holocene abrupt climate changes. *Proceedings of the National Academy of Sciences of the United States of America* 105: 13941–13946.
- Kaniewski D, Van Campo E, Paulissen E et al. (2011) The medieval climate anomaly and the Little Ice Age in coastal Syria inferred from pollen-derived palaeoclimatic patterns. *Global and Planetary Change* 78(3): 178–187.
- Karabacak V and Altunel E (2013) Evolution of the northern Dead Sea Fault Zone in southern Turkey. *Journal of Geodynamics* 65: 282–291.
- Karabacak V, Altunel E, Meghraoui M et al. (2010) Field evidences from northern Dead Sea Fault Zone (South Turkey). New findings for the initiation age and slip rate. *Tectonophysics* 480: 172–182.
- Kilic S, Evrendilek F, Berberoglu S et al. (2006) Environmental monitoring of land-use and land-cover changes in a Mediterranean region of Turkey. *Environmental Monitoring and Assessment* 114: 157–168.
- Kosmas C, Danalatos N, Cammeraat LH et al. (1997) The effect of land use on runoff and soil erosion rates under Mediterranean conditions. *Catena* 29: 45–59.
- Kuzucuoğlu C and Tsirtsoni Z (2016) Changements climatiques et comportements sociaux dans le passé: quelles corrélations? *Les Nouvelles De L'archéologie* 142: 49–55.
- Marathianou M, Kosmas C, Gerontidis S et al. (2000) Land-use evolution and degradation in Lesvos (Greece): A historical approach. *Land Degradation & Development* 11(1): 63–73.
- Margaris NS, Koutsidon E and Giourga C (1996) Changes in traditional Mediterranean land-use systems. In: Brandt CJ and Thornes J (eds) *Mediterranean Desertification and Land Use*. Chichester: Wiley, pp. 29–42.
- Meadows J (2005) The Younger Dryas episode and the radiocarbon chronologies of the Lake Huleh and Ghab Valley pollen diagrams, Israel and Syria. *The Holocene* 15: 631–636.
- Meghraoui M, Gomez F, Sbeinati R et al. (2003) Evidence for 830 years of seismic quiescence from palaeoseismology, archaeoseismology and historical seismicity along the Dead Sea fault in Syria. *Earth and Planetary Science Letters* 210(1): 35–52.
- Meyers PA and Teranes JL (2001) Sediment organic matter. In: Last WW and Smol JP (eds) *Tracking Environmental Change Using Lake Sediments*. Dordrecht: Kluwer Academic Publishers, pp. 239–269.
- Minyuk PS, Brigham-Grette J, Melles M et al. (2007) Inorganic geochemistry of El'gygytgyn Lake sediments (northeastern Russia) as an indicator of paleoclimatic change for the last 250 kyr. *Journal of Paleolimnology* 37(1): 123–133.
- Naveh Z and Dan J (ed.) (1973) *The Human Degradation of Mediterranean Landscapes in Israel*. Berlin; Heidelberg: Springer.
- Nesbitt IIW and Young GM (1982) Early Proterozoic climates and plate. *Nature* 299: 715–717.
- Nunes JP, Seixas J and Pacheco NR (2008) Vulnerability of water resources, vegetation productivity and soil erosion to climate change in Mediterranean watersheds. *Hydrological Processes* 22: 3115–3134.
- Parlak O, Rızaoğlu T, Bağcı U et al. (2009) Tectonic significance of the geochemistry and petrology of ophiolites in southeast Anatolia, Turkey. *Tectonophysics* 473: 173–187.
- Rich S (2013) *Ship Timber as symbol? Dendro-provenancing & contextualizing ancient cedar ship remains in the eastern Mediterranean*. PhD Thesis, KU Leuven.
- Robertson AHF (2002) Overview of the genesis and emplacement of Mesozoic ophiolites in the Eastern Mediterranean Tethyan region. *Lithos* 65: 1–67.
- Rowton MB (1967) The woodlands of ancient western Asia. *Journal of Near Eastern Studies* 26(4): 261–277.
- Schmidt S, Howa H, Mouret A et al. (2009) Particle fluxes and recent sediment accumulation on the Aquitanian margin of Bay of Biscay. *Continental Shelf Research* 29: 1044–1052.
- Schumm S (1963) Sinuosity of alluvial rivers on the Great Plains. *Geological Society of America Bulletin* 74: 1089–1100.
- Sorrel P and Mathis M (2016) Mid-to Late-Holocene coastal vegetation patterns in Northern Levant (Tell Sukas, Syria): Olive tree cultivation history and climatic change. *The Holocene* 26(6): 858–873.
- Sudom M and Arnaud JSR (1971) Use of quartz, zirconium and titanium as indices in pedological studies. *Canadian Journal of Soil Science* 51: 385–396.
- Talbot MR and Livingstone DA (1989) Hydrogen index and carbon isotopes of lacustrine organic matter as lake level indicators. *Palaeogeography, Palaeoclimatology, Palaeoecology* 70: 121–137.
- Tchalenko G (1953) *Villages antiques de la syrie du nord*. Paris: Éditions Geuthner.
- Van Andel TH, Zangger E and Demitrack A (1990) Land use and soil erosion in prehistoric and historical Greece. *Journal of Field Archaeology* 17: 379–396.
- Weiss B (1982) The decline of Late Bronze Age civilization as a possible response to climatic change. *Climatic Change* 4(2): 173–198.
- Welton L (2012) The Amuq Plain and Tell Tayinat in the third millennium BCE: The historical and socio-political context. *Canadian Society for Mesopotamian Studies* 6: 15–27.
- Wick L, Lemcke G and Sturm M (2003) Evidence of Lateglacial and Holocene climatic change and human impact in eastern Anatolia: High-resolution pollen, charcoal, isotopic and geochemical records from the laminated sediments of Lake Van, Turkey. *The Holocene* 13(5): 665–675.
- Wilkinson TJ (1997) The history of the Lake of Antioch: A preliminary note. In: Young G, Chavalas M and Averback R (eds) *Crossing Boundaries and Linking Horizons: Studies in Honor of Michael C. Potomac*, MD: CLD Press, pp. 557–576.
- Wilkinson TJ (1998) Water and human settlement in the Balikh Valley, Syria: Investigations from 1992–1995. *Journal of Field Archaeology* 25(1): 63–87.
- Wilkinson TJ (1999) Holocene Valley fills of Southern Turkey and Northwestern Syria: Recent geoarchaeological contributions. *Quaternary Science Reviews* 18: 555–571.
- Wilkinson TJ (2000) Geoarchaeology of the Amuq Plain. In: Yener AC, Harrison T, Verstraete J, et al. (eds) *The Amuq Valley Regional Project, 1995–1998*. *American Journal of Archaeology* 104: 168–179.
- Wilkinson TJ (2005) Soil erosion and valley fills in the Yemen highlands and southern Turkey: Integrating settlement, geoarchaeology, and climate change. *Geoarchaeology* 20: 169–192.
- Wilkinson TJ and Rayne L (2010) Hydraulic landscapes and imperial power in the near East. *Water History* 2: 115–144.

- Yasuda Y, Kitagawa H and Nakagawa T (2000) The earliest record of major anthropogenic deforestation in the Ghab Valley, northwest Syria: A palynological study. *Quaternary International* 73–74: 127–136.
- Yener KA (2005) Surveys in the plain of Antioch and Orontes Delta Turkey. In: Yener KA (ed.) *The Amuq Valley Regional Projects 1995–2002*. Chicago, IL: Oriental Institute Publications, pp. 1–24.
- Yener KA and Wilkinson TJ (2007) *The Amuq valley project 1995–96*. Chicago, IL: The Oriental Institute of the University of Chicago.
- Yener KA, Edens C, Harrison T et al. (2000) The Amuq valley regional project 1995–1998. *American Journal of Archaeology* 104: 163–220.
- Yener MS (2010) Turkish foundations in Cyprus. *Ankara Bar Review* 3: 121–124.
- Yönlü Ö, Altunel E, Karabacak V et al. (2010) Offset archaeological relics in the western part of the Büyük Menderes graben (western Turkey) and their tectonic implications. *Geological Society of America Special Papers* 471: 269–279.
- Zurcher EJ (2004) *Turkey: A Modern History*. New York: I.B. Tauris.